Fuel Processing Technology 173 (2018) 165–172

Contents lists available at ScienceDirect

Fuel Processing Technology

journal homepage: www.elsevier.com/locate/fuproc

Selective depolymerization of industrial lignin-containing stillage obtained from cellulosic bioethanol processing

Beatriz Gómez-Monedero[a,1], M. Pilar Ruiz[a,2], Fernando Bimbela[b,3], Jimmy Faria[a,*,4]

[a] Abengoa Research, Campus Palmas Altas, c/Energía Solar 1, 41014 Seville, Spain
[b] Grupo de Procesos Termoquímicos (GPT), Aragón Institute for Engineering Research (I3A), Universidad de Zaragoza, Mariano Esquillor s/n, 50018 Zaragoza, Spain

ARTICLE INFO

Keywords:
Lignin
Hydrogenolysis
Stillage
Carbon nanotubes
Depolymerization
1-D catalyst

ABSTRACT

Reductive depolymerization of lignin-containing stillage (LA lignin) from 2nd generation bioethanol industrial plants have been studied over two different families of catalysts: conventional porous Ru catalysts supported on ZrO_2 or activated carbon, and 1-dimensional Ru catalysts supported on multi-walled carbon nanotubes (MWCNT). The lignin depolymerization degree using conventional porous catalysts resulted in values of 42 and 53%, for Ru/ZrO_2 and Ru/C, respectively. Strikingly, when using 1D-supported catalysts (Ru/MWCNT and Ru/ZrO_2/MWCNT), the extent of lignin depolymerization measured by $^{1}H-^{13}C$ HSQC NMR, reached values of c.a. 80% of β-O-4 bond disappearance and a reduction of the average molecular weight from 3600 Da to ~ 1900 Da. The higher accessibility of the lignin agglomerates to the 1-D catalyst nanoparticles substantially improves the lignin depolymerization degree, which make this approach of great interest in the production of fine chemicals and fuel additives.

1. Introduction

The processing of lignocellulosic residues for producing bioethanol implies the treatment of biomass with microorganisms that transform two of its main fractions, cellulose and hemicellulose, into ethanol by fermentation [1]. A major challenge that remains unsolved, however, is the valorization of the lignin fraction, which is the most abundant natural source of aromatics. In many cases, lignin is obtained as a by-product that is used in biomass-boilers to generate heat [2,3]. Nonetheless, this approach has significant limitations, as lignin boilers are expensive and the energy content of this material is significantly lower than that of natural gas [4]. Additionally, the volume of lignin residue that will be produced readily exceeds the energy requirements of the biorefinery, complicating its utilization as energy source, unless electricity is generated and transferred to the electrical grid [5].

To date, significant efforts have been made in the development of homogeneous and heterogeneous catalysts for the valorization of lignin, most of them focused on the activation of the C—O bond [6–19]. Among the several ether bonds present in lignin, β-O-4 linkage is the most abundant and thus many studies have focused on the dissociation of such bond [20–23]. One major limitation of these approaches is the underestimation of the mass transport phenomena. It is well known that the driving force that determines the reaction rate is given by thermodynamic properties, such as chemical affinity, chemical potential, or activity [24,25]. Thus, when mass-transport effects, solvent competitive absorption, solvation of kinetically relevant reaction intermediates or catalyst deactivation are present, the system is not controlled by the surface reaction [26,27]. As a result, the basic knowledge on selective scission of C—O bonds of lignin model compounds becomes insufficient when scale-up is required, as mass transport and solvent-driven effects (deactivation and solvation) govern the kinetics of the process. In this sense, when comparing the particle size of globular lignin agglomerates (0.1 to 2 μm) with, for example, the pore size of activated carbon (2–50 nm) in which the active sites are located (*e. g.* metal clusters of 1–3 nm), it is obvious that most the catalyst surface is not being employed in the primary depolymerization steps. As a result, only the catalyst supported on the external surface will participate in the reaction, reducing the catalyst utilization dramatically in high-surface area supports. The remaining fraction of the catalyst will only catalyze secondary reactions of the dimers and trimers molecules that can

* Corresponding author.
E-mail address: j.a.fariaalbanese@utwente.nl (J. Faria).
[1] Department of Physical Chemistry, School of Industrial Engineers, University of Castilla-La Mancha, Campus Universitario s/n, 02071 Albacete, Spain.
[2] Sustainable Process Technology Group, Faculty of Science and Technology, University of Twente, 7500AE Enschede, The Netherlands.
[3] Grupo de Reactores Químicos y Procesos para la Valorización de Recursos Renovables, Institute for Advanced Materials (InaMat), Universidad Pública de Navarra, 31,006 Pamplona, Spain.
[4] Chemical Processes and Materials Group, Faculty of Science and Technology, MESA+ Institute for Nanotechnology, University of Twente, 7500AE Enschede, The Netherlands.

https://doi.org/10.1016/j.fuproc.2018.01.021
Received 20 November 2017; Received in revised form 14 January 2018; Accepted 25 January 2018

diffuse through the pores [28]. In contrast, homogeneous catalysts can readily reach most of the lignin C—O bonds with minimum mass transport limitations. However, the deactivation in aqueous environments and efficient recovery of these catalysts is a major challenge [29]. Thus, the development of new technologies that can combine the high stability and scalability of heterogeneous catalysts with the enhanced accessibility and chemical specificity of the homogeneous homologous could enable the industrial refining of lignin-streams in second generation biorefineries and paper-mill industries.

The present study is aimed at the development of one-dimensional (1D) catalytic materials that can penetrate the intricate lignin structure of industrially produced biomass stillage to activate the aryl-ether bonds for selective depolymerization. The concept is to use flexible one-dimensional materials as support for catalytic functionalities (metal nanoparticles) that can accomplish the hydrogenolysis of the linkage bonds in lignin. For this purpose, purified multi-walled carbon nanotubes (MWCNT) were selected as 1D support for Ru nanoparticles. Benchmarking of the Ru-based catalysts was performed to assess the effectiveness of the concept. The data from the reaction experiments was coupled with detailed characterization of the chemical and physical structure of the lignin-containing stillage to understand the underlying mechanism of reductive depolymerization.

2. Materials and methods

2.1. Lignin-containing stillage

The raw material used in catalytic depolymerization experiments was the solid obtained from the filtration of stillage from 2nd generation bioethanol production, referred as LA lignin. Stillage from 2nd generation bioethanol was provided by Abengoa Bioenergy. This stream consists of a heterogeneous mixture of suspended solids and partially solubilized organic matter in water. The process employed from which these samples are obtained can be found in several US Patents [30,31]. The feed was filtrated to obtain a solid residue also known as “cake” and the filtrate. The cake was dried and the solid recovered in such way was denoted as LA lignin.

2.2. Catalyst preparation and characterization

Materials acting as catalyst supports were either commercial or materials prepared or modified in the laboratory. Regarding commercial materials, activated carbon (Activated Charcoal DARCO®, ~100 mesh particle size, Sigma-Aldrich) and purified multi-walled carbon nanotubes (MWCNT-purified, kindly provided by SouthWest NanoTechnologies) were used. In addition, the following supports were prepared in the laboratory: zirconium oxide and ZrO_2/MWCNT. Other high purity chemicals and reagents were used for preparing the catalysts, which include the following: Zr(IV) oxynitrate hydrate 99%, $N_2O_7Zr.xH_2O$ (Sigma Aldrich), ammonia 28%, (VWR Chemicals), zirconium propoxide ($C_{12}H_{28}O_4Zr$) at a 70 vol% solution in propanol (Sigma-Aldrich), isopropanol (99.99% min. Purity, Sigma-Aldrich), and $RuCl_3$, 45–55% Ru content (Sigma-Aldrich). Further details about the preparation procedures of these catalysts can be found in the Supplementary Information and in a previous work [32]. Textural properties of some of these catalysts were analyzed by the following techniques: N_2 physisorption and high-resolution transmission electron microscopy (HRTEM). N_2 isotherms were determined at 77 K in an ASAP 2020 system (Micromeritics).

2.3. Lignin characterization

Different techniques were used for characterizing the raw material: elemental analysis, attenuated total reflectance infrared spectroscopy (ATR-IR), two-dimensional heteronuclear single quantum coherence spectroscopy (HSQC-2D), gel permeation chromatography (GPC), Klason determination of the lignin content, high-resolution transmission electron microscopy coupled with energy dispersive X-ray spectroscopy detector and electron energy loss spectroscopy (HRTEM-EDS-EELS), and scanning electron microscopy coupled with energy dispersive X-ray spectroscopy (SEM-EDS).

ATR spectra of LA lignin solid samples were acquired in a Bruker spectrometer, model VERTEX 70, equipped with a Platinum ATR module. 2D-NMR was performed in DMSO-d_6 on acetylated samples (acetylation procedure can be found on the Supplementary Information), to avoid fractionation of the material before NMR analysis and to increase both the solubility and the chemical shift dispersion of the side chain units. The inverse detected $^1H—^{13}C$ correlation spectra (HSQC) were measured at 25 °C on a Bruker AVANCE III 700 MHz instrument equipped with a cryogenically cooled 5mmTCI gradient probe with inverse geometry (proton coils closest to the sample). HSQC experiments used Bruker's “hsqcetgpsisp2.2” pulse program (adiabatic-pulsed version) with spectral widths of 5000 Hz (from 10 to 0 ppm) and 20,843 Hz (from 165 to 0 ppm) for the ^1H and ^{13}C dimensions. As LA lignin was obtained from the stillage of 2nd generation bioethanol production from corn stover, HSQC correlation peaks were assigned mainly by comparing with the study by Min et al. [33] on the structural changes of lignin and lignin-carbohydrate complexes in corn stover, though other references were also considered [34,35]. The degree of depolymerization was determined by gel permeation chromatography (modified Agilent 1260 Infinity).

The degree of depolymerization was determined by gel permeation chromatography (GPC, Hewlet Packard, Ti Series 1050). The GPC samples were prepared by dissolving 5 mg of acetylated lignin in tetrahydrofuran (THF) and the solution was filtered through a 0.2 μm syringe filter. The samples (20 μL) were injected into three PLgel 7.5 × 300 mm columns connected in series using an isocratic profile with THF as a mobile phase (1 mL/min) at 25 °C. The detection of the products was performed using a UV detector at 260 ± 40 nm. Calibration of the signal was done using polystyrene standards (Agilent S-L-10 with MW 162–20,000 g/mol).

HRTEM was carried out using a FEI Tecnai F30, operated at 300 kV equipped with a Gatan CCD camera, an EDS (EDAX) detector and a Gatan Tridiem Energy Filter for EELS characterization.

2.4. Reaction set-up

The laboratory-scale installation consisted of a high-pressure stainless-steel autoclave reactor equipped with a 50-mL teflon liner, a pressure transducer or two manometers (one for pressures up to 10 bar, the other for pressures up to 250 bar), a stainless-steel deposit for liquids, a thermocouple coupled to a temperature controller and a magnetic stirrer. Catalytic depolymerization of LA lignin was carried out by placing 50 mg of the desired catalyst inside the reactor vessel together with 500 mg of the lignin. Then, 30 mL of methanol were added to the reactor and it was subsequently sealed. A leak test was carried out by pressurizing with N_2 up to 50 bar-g. The reactor was then purged three times with H_2 to remove any N_2 left in the medium and then pressurized up to 25 bar using H_2. The relative centrifugal force was set to 4.55·g (750 rpm), and the temperature was increased from room temperature up to 200 °C in 120 min. Once the target temperature and pressure were reached (200 °C, 50 bar), the reaction time started. After the desired time of reaction, the heating and the stirring were stopped and the reactor was cooled down in an ice-cooled bath. When the temperature was under 20 °C, the reactor was depressurized.

2.5. Product characterization

After reaction, 1 mL of the liquid product was taken and filtered, using a syringe and a 45 μm syringe filter, and subsequently analyzed by GC–MS (Agilent 7890 GC-system, model G3440A, equipped with a 5975C mass spectrometer detector. Column: Agilent HP5-ms, 0.250 mm

inner diameter, 30 m long, 0.25 μm film thickness; or HP5, 0.320 mm inner diameter, 30 m long, 0.25 μm film thickness) to identify the products obtained. Then, the liquid product was also analyzed by GC-FID (Agilent 7890 GC-system, model G3440A, equipped with a 5975C flame ionization detector. Column: Agilent HP5) for quantification. The rest of the reaction mixture was centrifuged and the liquid fraction was collected in a flask. The solids were washed with methanol and ethyl acetate, centrifuged again and the liquid obtained after centrifugation was separated from the solids and added to the first liquid fraction collected in the flask. The liquid fraction was concentrated by rotary evaporation, eliminating methanol and ethyl acetate coming from reaction medium and washing. The remaining organics in the flask were weighed to quantify the mass of liquid products. The solids previously separated were also collected in a flask and dried in a rotary evaporator to eliminate any remaining solvent. The recovered solids were weighed, and the mass obtained represented the solid products together with the catalyst.

3. Results

3.1. Lignin characterization

Assessing the nanostructure of the stillage cake obtained from the industrial conversion of corn stover to ethanol was performed using HRTEM coupled with EDS (Supplementary Information). The material is highly heterogeneous, composed of elongated agglomerates connected by an amorphous film that resembles the structure of carbohydrates-lignin complexes [36]. Detailed characterization of the material by energy dispersive X-ray spectroscopy confirmed the presence of Ca, K, Si, Al, Ti, Fe, Mn, and Mg on the sample (Supplementary Information). These elements were found in large dense clusters, which most likely correspond to impurities and ash content in the biomass.

HSQC-2D spectra of acetylated LA lignin, together with the identification of relevant regions attributed to several substructures and types of linkages in the LA lignin employed in this work has been recently reported by our group [32]. Briefly, the regions corresponding to guaiacyl, syringyl, hydroxyphenyl units together with *p*-coumarate and ferulate structures were identified (Fig. 1). Some regions denoting the presence of methyl and methoxy groups can also be observed, attributed to the lignin structure itself and the acetylation step. The linkages that bond these units were identified as β-β or β-5, as well as β-O-4 ether linkages. To determine the extent of depolymerization after catalytic treatment of LA lignin, the regions corresponding to guaiacyl and syringyl units were employed in combination with β-O-4 linkages. By using the integral areas of each functional group contribution, it was possible to calculate the fraction of β-O-4 bonds. Notably, the results indicated that the raw material used in prior catalytic depolymerization studies contained 46.6% of β-O-4 bonds [32].

The compositional analysis of LA lignin showed that carbon, hydrogen, nitrogen, sulfur and oxygen concentrations were around 54, 6, 3, 0.4 and 38 wt%, respectively. Thus, it is possible to recognize that H, O and S concentrations of LA lignin were close to those previously reported for corn stover biomass [5,37,38]. However, the concentration of carbon was slightly higher. This increase could be attributed to the presence of highly aromatic structures of lignin, in agreement with HSQC and ATR data that indicate the presence of aromatic structures coupled, to some extent, *via* C-O-C bonds. Further indication of this is the Klason analysis of LA lignin, which showed that 58.8% of the stillage cake obtained from the cellulosic bioethanol production process is composed of lignin-like material.

3.2. Lignin reductive depolymerization

Different catalytic materials were studied for the depolymerization of LA lignin. The reactions were carried out at the following conditions: 4 h, 200 °C, 750 rpm, and 50 bar of H_2. The selected catalytic materials included: 5% Ru/ZrO_2, 5 wt% Ru/C, 5% Ru/MWCNT, and 5% Ru/ZrO_2/MWCNT.

The results obtained in preliminary tests indicated that on methanol reflux at 160 °C it was possible to reach 20% yield to liquids. The use of high temperatures (200 °C) increased the liquid yield to 38 and 48% in the absence of catalysts using N_2 or H_2 atmospheres, respectively. Using

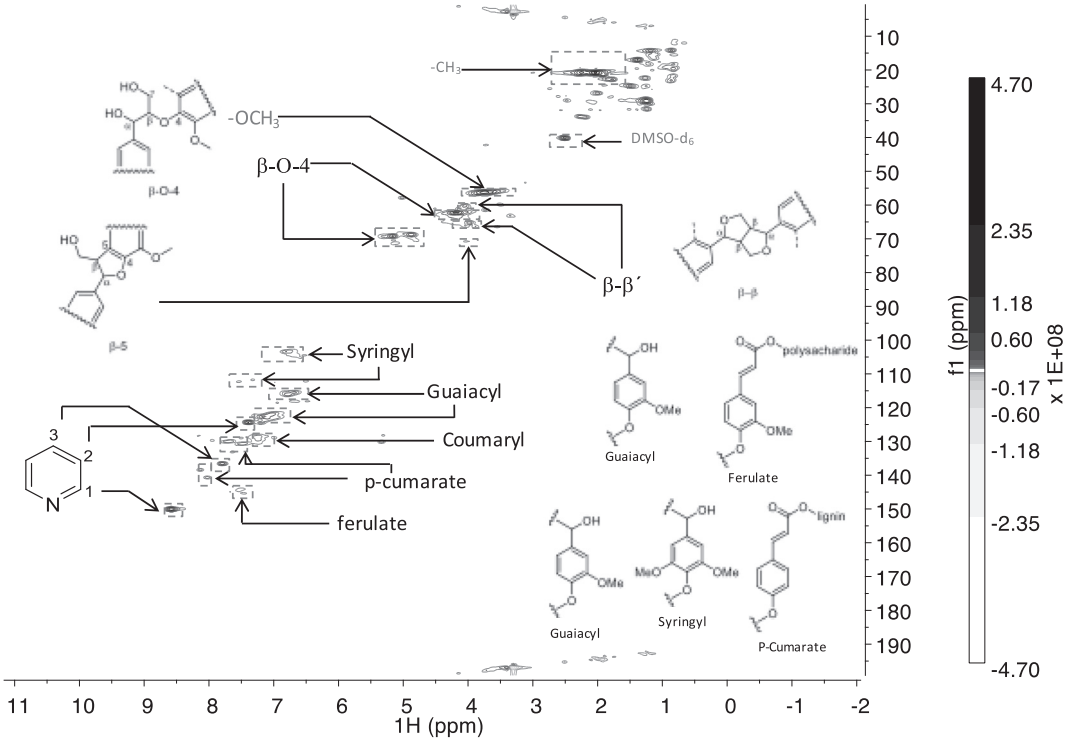

Fig. 1. HSQC-2D NMR of acetylated LA lignin indicating the different types of chemical bonds and monomers present in the system.

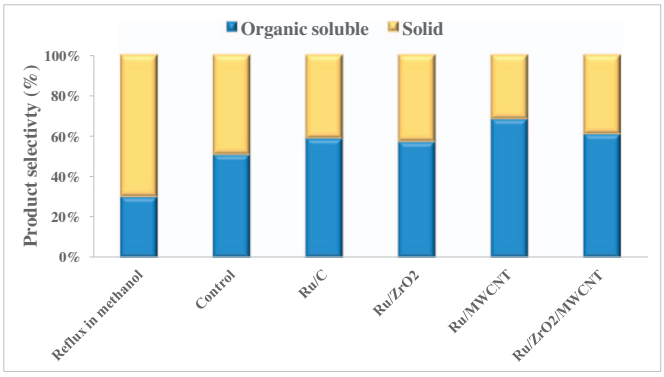

Fig. 2. Selectivity and mass balance of the organic soluble and solid products obtained after reaction LA lignin on different catalysts compared with the control (no catalyst) and LA lignin treated in methanol reflux at room pressure and 160 °C. Carbon mass balance was above 90 wt% in all the experiments.

5% Ru/C as catalyst for the reaction in H_2 the liquid yield increased to 55%, which is a small increase in the liquid yield. The high liquid yields observed using only methanol in N_2 and H_2 could be associated to either solvent-driven depolymerization or solvation of the polymers [39]. The yields to the corresponding solid and liquid products obtained in the catalytic tests are shown in Fig. 2.

The organic soluble selectivity obtained when the LA lignin was treated only in methanol in a reflux at 160 °C was rather significant, reaching 30 wt% after 4 h. This value increased up to 51% when the LA lignin was treated at 200 °C and 30 bar of H_2 in the absence of catalyst (control run). Upon the addition of catalyst, the organic soluble selectivity increased in all the experiments, reaching values above 57%. In terms of yield, Ru/C and Ru/ZrO_2 showed the highest productivities with values of 60 and 70 wt%, respectively, which are reasonably higher than the value obtained in the control experiment (55 wt%). While the presence of these catalysts seemed to favor the production of organic soluble products, the product yields were not substantially increased. Similar observations were reported by Anderson et al. [28] when treating corn stover in methanol under 30 bar of H_2 using Ni catalyst supported on carbon to perform the reductive fractionation of biomass. They observed a yield of 50 wt% to organic soluble oil after reaction using only activated carbon (*i.e.* control experiment).

5% Ru/MWCNT and 5% Ru/ZrO_2/MWCNT were used as catalysts to investigate the effect of catalyst shape on the reductive depolymerization of lignin. Both catalysts yielded similar results when referring to organic soluble and solid products (Fig. 2). Liquid yield increased from 51 wt% in the control experiment, to 68 and 61 wt% for Ru/MWCNT and Ru/ZrO_2/MWCNT, respectively. While the results were in the same range of values obtained with conventional porous catalysts, the product distribution and extent of depolymerization of β-O-4 bonds were substantially different.

To determine the extent of depolymerization, the solids obtained after reaction were analyzed by 2D NMR (Fig. 3). The characterization by $^{1}H-^{13}C$ HSQC NMR of these samples was centered at the region of 4.5 to 8.5 ppm (^{1}H) and 155 to 65 ppm (^{13}C). Here, it is possible to identify an intense peak at 6.6 to 7.4 ppm (^{1}H) and 120 to 125 ppm (^{13}C) assigned to guaiacyl. A lower intensity peak for guaiacyl was detected in the region of 6.2 to 6.6 ppm (^{1}H) and 115 to 120 ppm (^{13}C). The hydroxyphenyl peak was centered in the region of 6.6 to 7.0 ppm (^{1}H) and 125 to 130 ppm (^{13}C). The chemical shifts at 7.2 to 7.4 ppm (^{1}H) and 125 to 130 ppm (^{13}C) were assigned to p-coumarate. Also, the peak in the region 7.4 to 7.6 ppm (^{1}H) and 145 ppm (^{13}C) was assigned to p-coumarate. Ferulate was identified in the region 8.4 to 8.8 ppm (^{1}H) and 145 to 155 ppm (^{13}C). The characteristic ether bonds detected were β-o-4 and β-o-β'. The former was observed in the region of 4.8 to 5.4 ppm (^{1}H) and 65 to 75 ppm (^{13}C). The latter was detected in two regions. The chemical shifts at 4.5 to 4.7 ppm (^{1}H) and 65 to 70 ppm

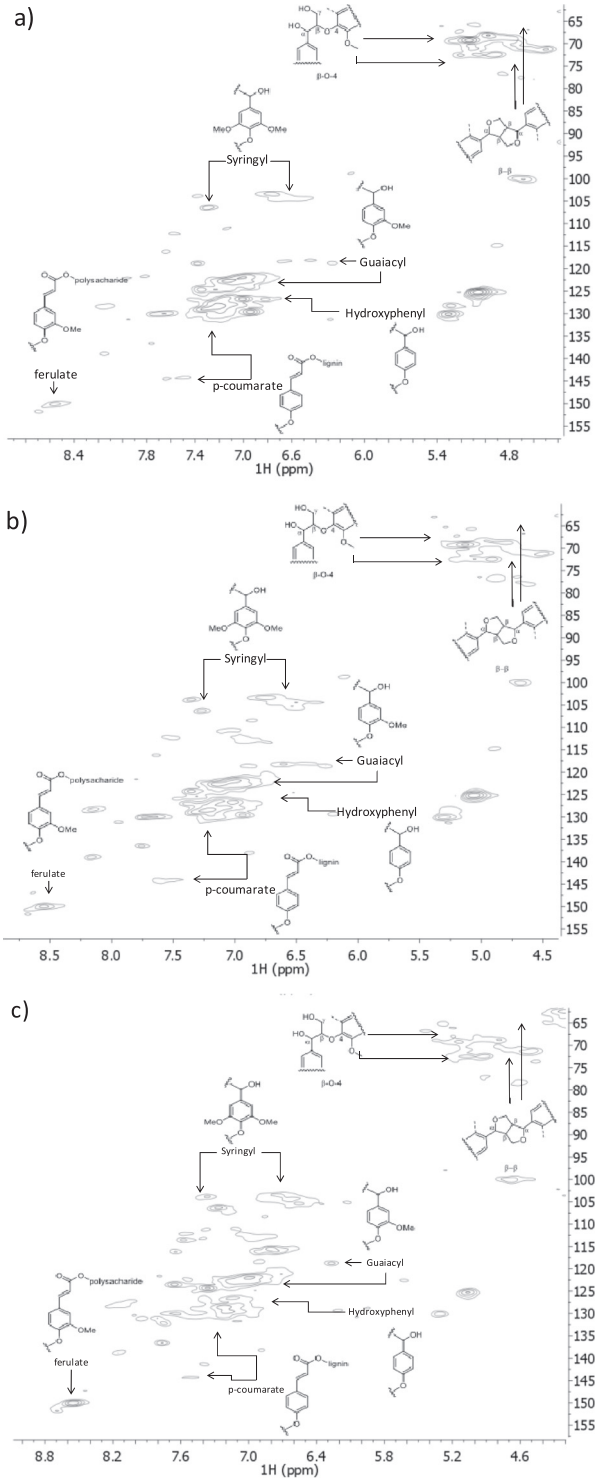

Fig. 3. 2D-NMR of acetylated LA lignin after 4 h of reaction at 200 °C and 50 bar of H_2 in methanol on Ru/ZrO_2 (a), Ru/C (b), and Ru/MWCNT (c) catalysts.

(^{13}C) and the region of 4.5 to 4.7 ppm (^{1}H) and 75 to 80 ppm (^{13}C). Notably, in all the samples most of these peaks were observed. However, the relative abundance of these signals was rather different. In this way, it was possible to determine the relative concentration of β-O-4 ether bonds in the samples.

The extent of β-O-4 disappearance was calculated using the change on the relative abundance of β-O-4 bond of LA lignin after the reaction (Table 1). It was previously shown that by treating lignin in N_2 or H_2 without the catalyst (reflux in methanol and control samples), the β-O-4

Table 1
Relative abundance of β-o-4, β-5 and β-β′ on the C9 units and extent of linkage disappearance obtained from 2D-NMR spectra integration of acetylated solids after reductive depolymerization.

Experiment	Relative abundance (%)/C_9			% disappearance		
	β-O-4	β-5	β-β′	β-O-4	β-5	β-β′
LA lignin	46.6	11.9	3.0	–		
Ru/C	21.9	8.9	2.4	53%	26%	20%
Ru/ZrO_2	27.1	10.7	2.9	42%	10%	4%
Ru/MWCNT	12.0	3.2	1.9	74%	73%	37%
Ru/ZrO_2/MWCNT	9.9	2.3	1.1	79%	81%	63%

depolymerization was only 7.4 and 10.3%, respectively [32]. While the solvation in methanol media was rather favorable as shown by the high liquid yields obtained in the reflux and control experiments (Fig. 2), the depolymerization of β-O-4 ether bonds was limited. In sharp contrast, the β-O-4 disappearance was 53% for the lignin solids after reaction in 5 wt% Ru/C. By using Ru/ZrO_2, it was possible to achieve a degree of depolymerization of β-O-4 ether bonds of 42%. This indicated that using heterogeneous catalysts it is possible to reach a 5-fold increase in the depolymerization of the LA lignin β-O-4 bonds.

Interestingly, it was observed that β-O-4 linkages in the sample after reaction with Ru/MWCNT accounted for around 12%, which means a reduction of *ca.* 74% when compared to the acetylated sample before reaction. This result indicates that supporting the catalyst in 1D nanomaterial enhanced the hydrogenolytic cleavage of the β-O-4 linkages in the lignin. Moreover, when the selected catalyst was Ru/ZrO_2/MWCNT, the percentage of bond disappearance of the target bonds increased up to 79%. This represents a 60% increase in the extent of depolymerization. Notably, the relative abundance of β-5 and β-β linkages in lignin also changed after reaction. Initially, the β-5 and β-β linkages represented 11.9 and 3%, respectively. Upon reaction on Ru catalyst supported on carbon (Ru/C), these values decreased to 8.9 and 2.4%, respectively. The disappearance of β-5 and β-β linkages in the solids after reaction increased significantly when Ru was supported on 1D carbon materials. For instance, when Ru/ZrO_2/MWCNT was used the disappearance of β-5 and β-β linkages reached values of 81 and 63%, respectively.

The high accessibility of the metal clusters to the lignin macromolecules could be the reason for this improvement in the depolymerization of lignin. In terms of surface area, Ru/MWCNT and Ru/ZrO_2/MWCNT have smaller surface areas than the activated carbon counterparts (300 *vs* 800 m^2/g). Most of the surface area of activated carbon, however, comes from its microporous structure (pore size < 2 nm), which limits the diffusion of lignin macromolecules. In contrast, the surface area of MWCNT could be divided in two contributions, the microporous surface corresponding to the inside of hollow multi-walled carbon nanotubes and the external surface area of the tubes. The latter will be rather accessible for the lignin polymers and oligomers. This in turn, resulted in a higher depolymerization activity.

The extent of depolymerization obtained by $^1H-^{13}C$ HSQC NMR was corroborated by the change in molecular weight distribution of the acetylated solids after reaction (Fig. 4). The molecular weight distribution of pristine LA lignin had four main features centered at 158, 300, 2300, and 8600 Da. That could correspond to monomers, dimers, oligomers, and large polymers. The average molecular weight of LA lignin before reaction was 3663 Da, with a polydispersion of 3.4. The addition of catalysts significantly reduced the intensity of the peak at the high molecular weight region (~8600 Da). In turn, new peaks at lower molecular weight region appeared, which are indicative of the reduction of molecular weight of LA lignin. The average molecular weight of the solids progressively decreased from 3663 Da to 2137 Da for Ru/C catalysts, respectively. In sharp contrast, the treatment of LA lignin in reflux at 160 °C drastically increased the average molecular

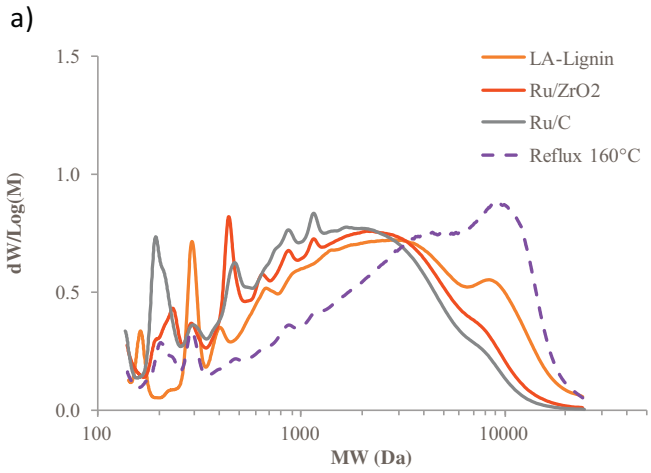

Fig. 4. Molecular weight distribution for the LA lignin depolymerization in reflux and over different catalysts at 200 °C, 50 bar of H_2.

weight, reaching 5083 Da. It is possible that in the presence of oxygen the coupling reactions of lignin oligomers to form larger polymeric structures were accelerated, explaining the increase in molecular weight. The high reactivity of lignin-containing oligomers has been previously reported [28].

The lowest molecular weight was obtained for Ru/MWCNT (~1900 Da). The number molecular weight (Mn) was around 1000 Da for all the samples, indicating that on fresh and depolymerized lignin the distribution of molecular weights is significantly broad. This observation was in line with high polydispersity values (between 2 and 3). While there are significant limitations in the use of gel permeation chromatography for the calculation of exact molecular weights of lignin samples, the trends observed here undoubtedly indicate the following; 1) addition of catalyst remarkably changed the molecular structure of lignin, and 2) catalyst micro-structure affects markedly the extent of depolymerization.

The GC–MS analysis of the samples showed a wide range of products (see Supplementary Information). Total concentration of detected compounds for each sample was calculated, obtaining the following results: 50.8 (Ru/ZrO_2), and 55.5 (Ru/C), 36 (Ru/MWCNT) and 35 (Ru/ZrO_2/MWCNT) g/L. The large fraction of unknown organic soluble products could be attributed to the formation oligomers dissolved in the liquid phase, which could have accounted for up to 80 wt% of total liquid products. As shown in Table 2, the product distribution was divided in four categories based on their molecular structure. The saturated monomers included the monomeric aromatic molecules with no unsaturated functionalities (toluene, benzene, phenol, 4-ethylphenol, 4-ethyl-2-methoxyphenol, 2,3-dihydrobenzofuran, o-methoxy-alfa-methylbenzyl alcohol, mandelic acid, methyl(3,4-dimethoxyphenyl) (hdroxy)acetate, methyl p-hydroxyhydrocinnamate, ethyl homovanillate). The unsaturated monomers included the aromatic compounds with unsaturated functional groups (trans-isoeugenol, 6-methoxyeugenol, methyl p-coumarate, methyl ferulate, 2-propenoic acid-3-

Table 2
Product distribution (wt%) obtained after 4 h of reductive depolymerization of lignin-containing stillage (LA lignin) at 200 °C and 30 bar of H_2 and 750 rpm.

Products	Catalysts		
	Ru/C	Ru/MWCNT	Ru/ZrO_2/MWCNT
Saturated monomers	10%	8%	7%
Unsaturated monomers	6%	5%	4%
Fatty acid esters	0%	0%	1%
Lactic acid byproducts	4%	0%	3%
Unknown	79%	87%	86%

(4-hydroxy-3-methoxyphenyl)-methyl ester). The fatty acid esters grouped the long chain esters that were detected in the product mixture after reaction (hexadecanoic acid methyl ester, hexadecanoic acid ethyl ester). Lactic acid byproducts included only lactic acid methyl ester.

Notably, the concentration of the detected compounds by GC-FID indicated that on Ru/MWCNT and Ru/ZrO_2/MWCNT a smaller concentration of products was obtained compared to conventional Ru/C (Table 2). Hence, the use of 1D catalytic materials favored the depolymerization of the β-O-4 linkages in LA lignin but, in turn, the yield to GC-detectable compounds was decreased. This seems to indicate that 1D structures favor the interaction of the active metal sites with bulk lignin, but further depolymerization of oligomers in the liquid phase occurred easily when conventional catalysts were used. Notably, the ratio of saturated to unsaturated monomers was nearly constant (*c.a.* 1.3 to 1.7) for conventional and 1D catalysts. This indicates that selectivity of the reaction is independent of the catalyst topology and chemistry.

According to STEM images of the catalysts (see Supplementary Information), Ru deposited in MWCNT presented a mean particle size of 2.6 nm, whereas the mean pore diameter of the internal channels of MWCNT is in the 4 nm range. This could have caused that some of the metal particles were deposited inside the nanotubes channels, and thus being inaccessible for lignin aggregates and oligomers for reaction. Conversely, in ZrO_2/MWCNT the impregnation of ZrO_2 onto the nanotubes could have caused the blockage of some of these pores, or the reduction of their channel diameter. The reduction of BET area observed for this catalyst (31 m^2/g) when compared to 5% Ru/MWCNT (301 m^2/g) seems to support this. Thus, if the internal channels of the MWCNT are blocked to some extent, more active metal will be deposited onto the surface of the material during impregnation. Consequently, more active metal sites will be accessible for bulk lignin depolymerization and for the oligomers to undergo further reaction.

4. Discussion

Industrial lignin-containing stillage possesses a significant concentration of lignin macromolecules with a high concentration of β-O-4 ether bonds (47%) that connected individual aromatic units of the polymer. As shown in Scheme 1, to effectively breakdown the structure of the lignin it is necessary to access individual C—O bonds and activate the hydrogenolytic scission selectively. This in turn will generate oligomers and low molecular weight molecules that can undergo further hydrogenation. In parallel, these macromolecules could undergo solvolysis in methanol [40–47]. This will lead to the formation of unsaturated oligomers and monomers that can undergo rapid repolymerization if the highly reactive functionalities of the aromatic molecules are not promptly passivated [28]. The results herein reported indicated that in the presence of catalyst and reductive environment the lignin-containing stillage can be effectively transformed into monomeric and oligomeric products. The yield of organic products and detectable monomers in the GC–MS showed significant improvements compared to the control experiments, which clearly indicates that the utilization of catalysts improved the product yield. However, the use of different catalysts had very little effect on the productivity and selectivity on the reductive depolymerization in the liquid phase. This could be associated to mass transport limitations, where the catalyst is not participating directly on the activation of C—O ether linkages of the LA lignin [15,16,48]. Alternatively, it could be possible that a significant fraction of the catalytic activity observed takes place in the homogeneous phase. For instance, highly reducing species formed on the catalyst surface could be rapidly desorbed and diffused to the reaction media to unselectively attack the lignin polymers. However, 2D–NMR data showed that in fact the depolymerization process was selective. In the presence of catalysts, the disappearance of β-O-4 linkages was markedly enhanced and no other hydrogenation products were observed. Therefore, one could state that this process was not random, like radical reactions, but concerted. Thus, the catalysts catalyzed the selective C—O cleavage by hydrogenolysis. Interestingly, the extent of hydrogenolysis was sensitive to the shape of the catalyst support. When Ru was supported on 1D materials (*e.g.* MWCNT and ZrO_2/MWCNT) the disappearance of β-O-4 linkages increased to 75–80%, compared to the 50% achieved using Ru/C and 20% observed in the control experiment. This enhancement could be attributed to the higher accessibility of the catalysts as the metal clusters are directly exposed to the reaction media, instead of being confined inside the microporous structure of the catalyst.

While the higher disappearance of C—O ether bonds should result in an increase on organic soluble yield and monomers concentration, it

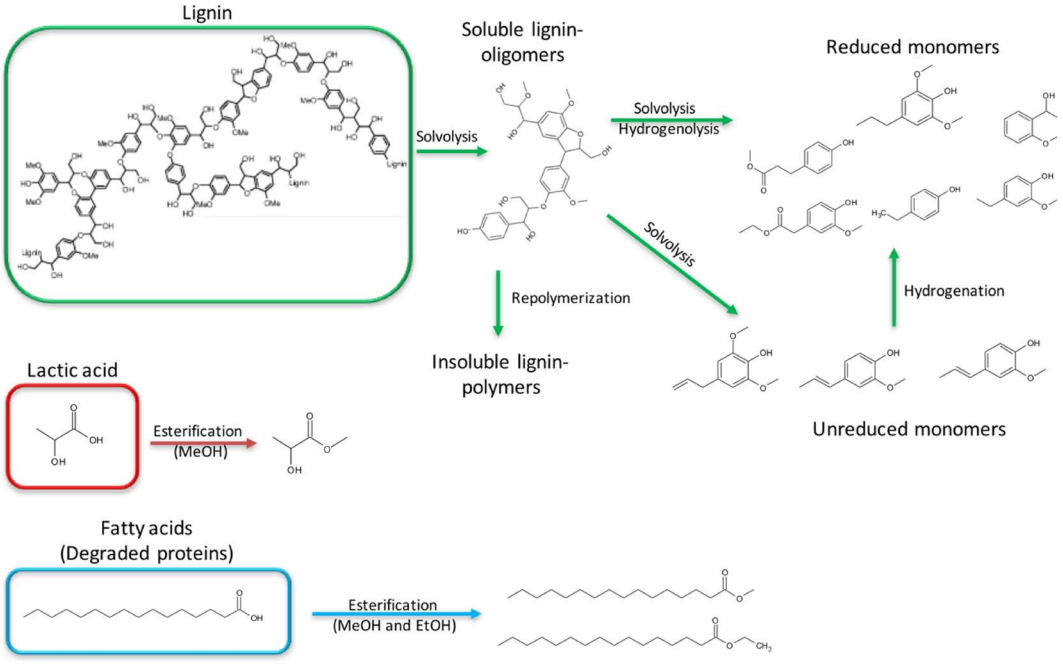

Scheme 1. Reaction scheme for the reductive depolymerization of lignin-containing stillage derived from cellulosic bioethanol process.

could be possible that after C—O hydrogenolysis lignin fragments could undergo repolymerization on the reaction media. The reflux experiment in methanol showed that in the presence of oxygen at mild temperatures it is possible to repolymerize the lignin oligomers and monomers to form high-molecular weight polymers. It could be proposed that as the reaction proceeds the concentration of lignin-oligomers increases, which in turn favors the undesired recombination of lignin. This will lead to asymptotic yields of liquid products and possible catalyst fouling due to carbon deposition. Alternatively, it is possible that as the LA lignin macromolecular structure is being depolymerized, the products of the reaction reabsorb on the catalyst surface blocking the active sites. These effects can be substantially accelerated on the 1D catalyst as its highly accessible surface will facilitate the diffusion and adsorption of large lignin macromolecules and oligomers. Multiple-site chemisorption, Van der Waals dispersion forces, and hydrogen bonding interactions between MWCNT and lignin polymers could further increase the catalyst deactivation. This could explain the greater extent of depolymerization of β-O-4 and lower molecular weight observed in the lignin after reaction, accompanied by a lower concentration of organic soluble products. Thus, it can be envisioned that optimization of the catalyst-lignin interaction and increasing the accessibility of the catalyst could drastically improve the liquid yields and monomers productivity.

5. Conclusions

In this work, we have studied the conversion of industrial lignin-containing stillage derived from 2nd generation ethanol plants. This is a rich-lignin solid with a high concentration of β-O-4 ether bonds (47%), which conversion has been our main target in this study. By developing 1-dimensional catalysts we have been able to significantly improve (up to 80%) the disappearance of these linkages, in comparison to conventional catalysts. This enhancement in lignin depolymerisation, boosted mainly by the better accessibility of the lignin macromolecules to the catalyst active sites, may be a starting point to develop future technologies aimed at converting lignin into added value chemicals, such as fuel additives.

Acknowledgements

The authors would like to thank the European Union (Project Valor Plus funded under the EU's Seventh Framework Programme, project FP7-KBBE-2013-7-613802). The authors would like to acknowledge the use of Servicio General de Apoyo a la Investigación-SAI at the Universidad de Zaragoza, particularly the assistance provided by the Servicio de Microscopia Electrónica de Materiales. The authors greatly appreciate the insightful comments and discussions of Prof. J. Arauzo and Prof. D. E. Resasco on lignin valorization and catalytic conversion.

Appendix A. Supplementary data

Supporting information available with further details on the experimental procedures and the characterization results. Supplementary data associated with this article can be found in the online version, at doi: https://doi.org/10.1016/j.fuproc.2018.01.021.

References

[1] J.M. Salgado, L. Abrunhosa, A. Venâncio, J.M. Domínguez, I. Belo, Enhancing the bioconversion of winery and olive mill waste mixtures into Lignocellulolytic enzymes and animal feed by aspergillus uvarum using a packed-bed bioreactor, J. Agric. Food Chem. 63 (2015) 9306–9314, http://dx.doi.org/10.1021/acs.jafc.5b02131.

[2] V. Menon, M. Rao, Trends in bioconversion of lignocellulose: biofuels, platform chemicals & biore fi nery concept, Prog. Energy Combust. Sci. 38 (2012) 522–550, http://dx.doi.org/10.1016/j.pecs.2012.02.002.

[3] R. Parajuli, T. Dalgaard, U. Jorgensen, A.P.S. Adamsen, M.T. Knudsen, M. Birkved, M. Gylling, J.K. Schjorring, U. Jorgensen, A.P.S. Adamsen, M.T. Knudsen, M. Birkved, M. Gylling, J.K. Schjorring, Biorefining in the prevailing energy and materials crisis: a review of sustainable pathways for biorefinery value chains and sustainability assessment methodologies, Renew. Sust. Energ. Rev. 43 (2015) 244–263, http://dx.doi.org/10.1016/j.rser.2014.11.041.

[4] M. Naqvi, J. Yan, E. Dahlquist, Black liquor gasification integrated in pulp and paper mills: a critical review, Bioresour. Technol. 101 (2010) 8001–8015, http://dx.doi.org/10.1016/j.biortech.2010.05.013.

[5] R.V. Morey, D.L. Hatfield, R. Sears, D. Haak, D.G. Tiffany, N. Kaliyan, Fuel properties of biomass feed streams at ethanol plants, Appl. Eng. Agric. 25 (2009) 57–64, http://dx.doi.org/10.13031/2013.25421.

[6] X. Zhang, Q. Zhang, J. Long, Y. Xu, T. Wang, Y. Li, Phenolics production through catalytic depolymerization of alkali lignin with metal chlorides, Bioresources 9 (2014) 3347–3360.

[7] X. Zhang, Q. Zhang, T. Wang, L. Ma, Y. Yu, L. Chen, Hydrodeoxygenation of lignin-derived phenolic compounds to hydrocarbons over Ni/SiO2-ZrO2 catalysts, Bioresour. Technol. 134 (2013) 73–80, http://dx.doi.org/10.1016/j.biortech.2013.02.039.

[8] X. Zhang, Q. Zhang, T. Wang, B. Li, Y. Xu, L. Ma, Efficient upgrading process for production of low quality fuel from bio-oil, Fuel 179 (2016) 312–321, http://dx.doi.org/10.1016/j.fuel.2016.03.103.

[9] W. Xu, S.J. Miller, P.K. Agrawal, C.W. Jones, Depolymerization and hydrodeoxygenation of switchgrass lignin with formic acid, ChemSusChem 5 (2012) 667–675, http://dx.doi.org/10.1002/cssc.201100695.

[10] S. Nanayakkara, A.F. Patti, K. Saito, Chemical depolymerization of lignin involving the redistribution mechanism with phenols and repolymerization of depolymerized products, Green Chem. 16 (2014) 1897–1903, http://dx.doi.org/10.1039/c3gc41708e.

[11] Q. Song, F. Wang, J. Xu, Hydrogenolysis of lignosulfonate into phenols over heterogeneous nickel catalysts, Chem. Commun. 48 (2012) 7019, http://dx.doi.org/10.1039/c2cc31414b.

[12] Q. Song, F. Wang, J. Cai, Y. Wang, J. Zhang, W. Yu, J. Xu, Lignin depolymerization (LDP) in alcohol over nickel-based catalysts via a fragmentation-hydrogenolysis process, Energy Environ. Sci. 6 (2013) 994–1007.

[13] C. Li, X. Zhao, A. Wang, G.W. Huber, T. Zhang, Catalytic transformation of lignin for the production of chemicals and fuels, Chem. Rev. 115 (2015) 11559–11624, http://dx.doi.org/10.1021/acs.chemrev.5b00155.

[14] S. Zhang, Conversion of lignin model compounds under mild conditions in pseudo-homogeneous systems, Green Chem. 18 (2016) 2341–2352, http://dx.doi.org/10.1039/c5gc03121d.

[15] A. Narani, R.K. Chowdari, C. Cannilla, G. Bonura, F. Frusteri, H.J. Heeres, K. Barta, Efficient catalytic hydrotreatment of Kraft lignin to alkylphenolics using supported NiW and NiMo catalysts in supercritical methanol, Green Chem. 17 (2015) 5046–5057, http://dx.doi.org/10.1039/C5GC01643F.

[16] K. Barta, H. Jan, C.R. Kumar, N. Anand, A. Kloekhorst, C. Cannilla, G. Bonura, F. Frusteri, K. Barta, H.J. Heeres, Solvent free depolymerization of Kraft lignin to alkyl-phenolics using supported NiMo and CoMo catalysts, Green Chem. 17 (2015) 4921–4930, http://dx.doi.org/10.1039/C5GC01641J.

[17] X. Wang, R. Rinaldi, A route for lignin and bio-oil conversion, Dehydroxylation of phenols into arenes by Catalytic Tandem Reactions.pdf, 2013.

[18] W. Schutyser, S. Van Den Bosch, J. Dijkmans, S. Turner, M. Meledina, G. Van Tendeloo, D.P. Debecker, B.F. Sels, Selective nickel-catalyzed conversion of model and lignin-derived phenolic compounds to cyclohexanone-based polymer building blocks, ChemSusChem 8 (2015) 1805–1818, http://dx.doi.org/10.1002/cssc.201403375.

[19] S. Van den Bosch, W. Schutyser, R. Vanholme, T. Driessen, S.-F. Koelewijn, T. Renders, B. De Meester, W.J.J. Huijgen, W. Dehaen, C.M. Courtin, B. Lagrain, W. Boerjan, B.F. Sels, Reductive lignocellulose fractionation into soluble lignin-derived phenolic monomers and dimers and processable carbohydrate pulps, Energy Environ. Sci. 8 (2015) 1748–1763, http://dx.doi.org/10.1039/C5EE00204D.

[20] B. Gomez-Monedero, J. Faria, F. Bimbela, M.P. Ruiz, Catalytic hydroprocessing of lignin β-O-4 ether bond model compound phenethyl phenyl ether over ruthenium catalysts, Biomass Convers. Biorefinery. (2017), http://dx.doi.org/10.1007/s13399-017-0275-5.

[21] T.H. Parsell, B.C. Owen, I. Klein, T.M. Jarrell, C.L. Marcum, L.J. Haupert, L.M. Amundson, H.I. Kenttämaa, F. Ribeiro, J.T. Miller, M.M. Abu-Omar, Cleavage and hydrodeoxygenation (HDO) of C–O bonds relevant to lignin conversion using Pd/Zn synergistic catalysis, Chem. Sci. 4 (2013) 806–813, http://dx.doi.org/10.1039/c2sc21657d.

[22] K. Barta, G.R. Warner, E.S. Beach, P.T. Anastas, Depolymerization of organosolv lignin to aromatic compounds over cu-doped porous metal oxides, Green Chem. 16 (2014) 191–196, http://dx.doi.org/10.1039/c3gc41184b.

[23] C.S. Lancefield, O.S. Ojo, F. Tran, N.J. Westwood, Isolation of functionalized phenolic monomers through selective oxidation and C-O bond cleavage of the b-O-4 linkages in lignin, Angew. Commun. 54 (2015) 258–262, http://dx.doi.org/10.1002/anie.201409408.

[24] J.P. Oconnell, M. Boudart, Catalytic hydrogenation of cyclohexene, AICHE J. 24 (1978) 904–911.

[25] R.J. Madon, E. Iglesia, Catalytic reaction rates in thermodynamically non-ideal systems, J. Mol. Catal. A Chem. 163 (2000) 189–204, http://dx.doi.org/10.1016/S1381-1169(00)00386-1.

[26] S. Mukherjee, M.A. Vannice, Solvent effects in liquid-phase reactions II. Kinetic modeling for citral hydrogenation, J. Catal. 243 (2006) 131–148, http://dx.doi.org/10.1016/j.jcat.2006.06.018.

[27] S. Mukherjee, M.A. Vannice, Solvent effects in liquid-phase reactions. I. Activity and selectivity during citral hydrogenation on Pt/SiO2 and evaluation of mass transfer effects, J. Catal. 243 (2006) 108–130, http://dx.doi.org/10.1016/j.jcat.2006.06.

021.
[28] E.M. Anderson, R. Katahira, M. Reed, M.G. Resch, E.M. Karp, G.T. Beckham, Y. Román-Leshkov, Reductive catalytic fractionation of corn Stover lignin, ACS Sustain. Chem. Eng. 4 (2016) 6940–6950, http://dx.doi.org/10.1021/acssuschemeng.6b01858.
[29] W. Keim, Multiphase catalysis and its potential in catalytic processes: the story of biphasic homogeneous catalysis, Green Chem. 5 (2003) 105–111 (doi:10.1039/b300138p).
[30] Q.A. Nguyen, W. He, D.L. Holmes, Methods for Controling Pretreatment of Biomass, US 2014/0083939 A1, (2014).
[31] Q.A. Nguyen, Method for producing ethanol, and co-products from cellulosic biomass, EP 2767633 (2014) A1.
[32] B. Gómez-Monedero, M.P. Ruiz, F. Bimbela, J. Faria, Selective hydrogenolysis of α–O–4, β–O–4, 4–O–5 C–O bonds of lignin-model compounds and lignin-containing stillage derived from cellulosic bioethanol processing, Appl. Catal. A Gen. 541 (2017) 60–76, http://dx.doi.org/10.1016/j.apcata.2017.04.022.
[33] D.Y. Min, H. Jameel, H.M. Chang, L. Lucia, Z.G. Wang, Y.C. Jin, The structural changes of lignin and lignin–carbohydrate complexes in corn stover induced by mild sodium hydroxide treatment, RSC Adv. 4 (2014) 10845–10850, http://dx.doi.org/10.1039/c3ra47032f.
[34] T.Q. Yuan, F. Xu, R.C. Sun, Role of lignin in a biorefinery: separation characterization and valorization, J. Chem. Technol. Biotechnol. 88 (2013) 346–352, http://dx.doi.org/10.1002/jctb.3996.
[35] J.L. Wen, S.L. Sun, B.L. Xue, R.C. Sun, Recent advances in characterization of lignin polymer by solution-state nuclear magnetic resonance (NMR) methodology, Materials (Basel). 6 (2013) 359–391, http://dx.doi.org/10.3390/ma6010359.
[36] B.S. Donohoe, S.R. Decker, M.P. Tucker, M.E. Himmel, T.B. Vinzant, Visualizing lignin coalescence and migration through maize cell walls following thermochemical pretreatment, Biotechnol. Bioeng. 101 (2008) 913–925, http://dx.doi.org/10.1002/bit.21959.
[37] A. Kumar, L. Wang, Y.A. Dzenis, D.D. Jones, M.A. Hanna, Thermogravimetric characterization of corn stover as gasification and pyrolysis feedstock, Biomass Bioenergy 32 (2008) 460–467, http://dx.doi.org/10.1016/j.biombioe.2007.11.004.
[38] A. Demirbas, Calculation of higher heating values of biomass fuels, Fuel 76 (1997) 431–434, http://dx.doi.org/10.1016/S0016-2361(97)85520-2.
[39] B. Gómez-Monedero, M.P. Ruiz, F. Bimbela, J. Faria, Selective hydrogenolysis of α-O-4, β-O-4, 4-O-5 CO bonds of lignin-model compounds and lignin-containing stillage derived from cellulosic bioethanol processing, Appl. Catal. A Gen. 541 (2017) 60–76, http://dx.doi.org/10.1016/j.apcata.2017.04.022.
[40] C. Zhao, J.A. Lercher, Catalytic depolymerization and deoxygenation of lignin, Role Catal. Sustain. Prod. Bio-Fuels Bio-Chemicals, 2013, pp. 289–320 (doi:10.1016/B978-0-444-56330-9.00009-7).
[41] S. Kasakov, H. Shi, D.M. Camaioni, C. Zhao, E. Baráth, A. Jentys, J.a. Lercher, Reductive deconstruction of organosolv lignin catalyzed by zeolite supported nickel nanoparticles, Green Chem. 17 (2015) 5079–5090, http://dx.doi.org/10.1039/C5GC02160J.
[42] R. Beauchet, F. Monteil-Rivera, J.M. Lavoie, Conversion of lignin to aromatic-based chemicals (L-chems) and biofuels (L-fuels), Bioresour. Technol. 121 (2012) 328–334, http://dx.doi.org/10.1016/j.biortech.2012.06.061.
[43] J. Horacek, F. Homola, I. Kubickova, D. Kubicka, Lignin to liquids over sulfided catalysts, Catal. Today 179 (2012) 191–198, http://dx.doi.org/10.1016/j.cattod.2011.06.031.
[44] R.J.A. Gosselink, W. Teunissen, J.E.G. van Dam, E. de Jong, G. Gellerstedt, E.L. Scott, J.P.M. Sanders, Lignin depolymerisation in supercritical carbon dioxide/acetone/water fluid for the production of aromatic chemicals, Bioresour. Technol. 106 (2012) 173–177, http://dx.doi.org/10.1016/j.biortech.2011.11.121.
[45] F. Behrendt, Y. Neubauer, M. Oevermann, B. Wilmes, N. Zobel, Direct liquefaction of biomass, Chem. Eng. Technol. 31 (2008) 667–677, http://dx.doi.org/10.1002/ceat.200800077.
[46] J. Zakzeski, P.C.A. Bruijnincx, A.L. Jongerius, B.M. Weckhuysen, The catalytic valorization of lignin for the production of renewable chemicals, Chem. Rev. 110 (2010) 3552–3599, http://dx.doi.org/10.1021/cr900354u.
[47] H. Wang, M. Tucker, Y. Ji, Recent development in chemical Depolymerization of lignin: a review, J. Appl. Chem. 2013 (2013) 1–9, http://dx.doi.org/10.1155/2013/838645.
[48] A.L. Jongerius, P.C. a. Bruijnincx, B.M. Weckhuysen, Liquid-phase reforming and hydrodeoxygenation as a two-step route to aromatics from lignin, Green Chem. 15 (2013) 3049. (doi:10.1039/c3gc41150h).